An Experimental and Modeling Study of Softening Coal Pyrolysis

A quantitative model of softening coal pryolysis is developed and tested against observed behavior. The model treats intraparticle transport of gases and metaplast throughout the softening stage of pyrolysis via growth of bubbles uniformly dispersed in the molten coal. The model quantitatively describes the transient softening behavior including the initiation, duration, and magnitude of plasticity and swelling of the particle. The model kinetic parameters are derived from experiments, in which a highly softening Pittsburgh No. 8 bituminous coal was pyrolyzed, and total weight loss, and yields and molecular weight distributions of tars and pyridine extractables of cooled chars were measured. Model predictions of effects of pressure, particle diameter and temperature on tar yields and weight losses, of effects of pressure on swelling ratio, and of effects of heating rate on plasticity are presented. The model provides good fits to the laboratory data and predicts trends in pyrolysis behavior in good qualitative accord with expectations based on published data.

Myongsook S. Oh
William A. Peters
Jack B. Howard
Energy Laboratory and
Department of Chemical Engineering
Massachusetts Institute of Technology
Cambridge, MA 02139

Introduction

Volatile products of coal pyrolysis are generated through the coal matrix, and the distribution and yield of pyrolysis products can be influenced by transport and chemical reactions of the volatiles within and outside the coal particle. Quantitative modeling of pyrolysis, therefore, requires analysis of intra- and extra-particle transport and chemical reactions. For softening coals, the problem is complicated by the fact that the modes of volatiles transport are strongly influenced by the softening behavior. This contrasts nonplastic coals that maintain a relatively unchanged open porous structure throughout pyrolysis, thus allowing volatiles transport to the particle surface via diffusion and hydrodynamic flow through pores.

The structural changes in plastic coals are radicals, involving successive transformation of the decomposing matrix from a solid to a solid-liquid-gaseous mixture, and finally to a resolidified phase. The intermediate solid-liquid-gaseous stage arises when plastic coals soften to form a fluid-like viscous mass that can be described as a mixture of unsoftened coal constituents (mineral matter and certain nonsoftening macerals) in an organic liquid continuum, throughout which pyrolysis-derived volatiles form bubbles. Because of the high viscosity of molten coal, bubble movement due to buoyancy is negligible but the bubbles grow by diffusive influx of volatiles from the coal melt. Transportable heavy hydrocarbons or tar species formed within the molten coal evaporate into the bubbles or diffuse through the coal melt and evaporate at the particle surface. Some of these species may undergo secondary reactions to form lighter and heavier products.

It is difficult to mathematically formulate the coupled effects of transport and chemistry under softening conditions. Furthermore, there is a severe lack of experimental data on the physicochemical phenomena contributing to the structural modifications, including the rheological behavior of softened coal, volatiles secondary reactions, and the effects of reaction conditions on the intraparticle inventory of coal plasticizing agent, metaplast (Van Krevelen, 1961; Neavel, 1982). Considerable progress has been made in modeling intraparticle volatiles transport in the pyrolysis of nonsoftening coals (Russel et al., 1979; Chen and Wen, 1979; Gavalas and Wilkes, 1980). There has been much less headway for softening coals, despite valuable contributions (Lewellen, 1975; Mills et al., 1976; James and Mills, 1976). For softened coals, volatiles transport is often described solely in terms of pseudosteady-state evaporation at the particle surface (Suuberg et al., 1979; Unger and Suuberg, 1981; Zacharias, 1979), thereby ignoring intraparticle transport

Present Address of M. S. Oh is Lawrence Livermore National Laboratory, P.O. Box 808, Livermore, CA 94550.
Correspondence concerning this paper should be addressed to J. B. Howard.

limitations. However, characteristic time analyses by Oh (1985), summarized below, show that, for pressures and particle sizes of interest in coal processing, intra-partricle volatiles transport resistance greatly exceeds that for evaporative (boundary layer) transport.

The need for further progress on intraparticle transport modeling is pressing especially for softening coals since they show the strongest influence of mass transport processes as evidenced by the effects of pressure and, to a lesser extent, particle size on their pyrolysis product yields and compositions (Anthony and Howard, 1976; Suuberg, 1977; Howard, 1981; Bleik et al., 1985; Wagner et al., 1985; Bautistu et al., 1986). The present paper responds to this need by providing a mathematical model of softening coal pyrolysis that includes intraparticle chemical reactions and volatiles transport. The model also accounts for changes in the coal structure during pyrolysis including plasticity and swelling. Experiments are performed to provide kinetic information on metaplast formation and decomposition reactions, and to measure molecular weight distribution of metaplast, both transported out of and remaining in the particle, in order to characterize the processes responsible for metaplast transport. Use of the model is illustrated via predictions of volatiles yields, transient plasticity, and swelling behavior.

Experiments

Defining metaplast

The precise physico-chemical nature of coal-derived metaplast remains to be established. Here, metaplast is viewed as pyrolysis-derived coal tar that has not evaporated, either into bubbles or from the particle surface. The weight of material recoverable by pyridine extraction of the char remaining after the coal has undergone a given extent of pyrolysis is taken as a measure, at that extent of pyrolysis, of total inventory of metaplast in the condensed phase plus tar vapor in the bubble phase. The corresponding molecular weight distribution (MWD) of the pyridine extract is taken as the MWD for metaplast plus tar in bubbles.

Pyrolysis

The coal was pyrolyzed in a batch electrical screen-heater reactor for which design details and operating procedures are given elsewhere (Oh, 1985; Caron, 1979). The reactor is designed for pyrolysis measurements of relatively large samples compared to the one in previous studies (Anthony, 1974; Suuberg, 1978; Franklin, 1980) and is not equipped with a liquid-nitrogen quench as in the reactor by Fong (1986a). Thin layers of about 35-40 mg of powdered Pittsburgh No. 8 Seam bituminous coal (75–90 μm particle diameter) were spread between the bottom folds of preweighed, triply-folded 325 mesh stainless steel screen, and heated under helium at pressures of 1 atm and approximately 0.0001 atm (vacuum). The temperature-time history of the coal particles throughout each run was measured by a chromel-alumel thermocouple (24 μm wire dia, and 75 μm bead dia.) inserted within the screen and connected to a fast response recorder. The temperature-time history consisted of a linear heat up to a prescribed peak temperature followed immediately by natural cooling via radiation, conduction and convection. The heating rate was 1,000°C/s and the peak temperatures were between 200°C and 1,050°C.

In previous studies, char was defined as the condensed-phase product retained on the screen upon completion of the run. Here, this product was further divided into extract removed by Soxhlet extraction in pyridine and the residue. Tar was operationally defined as materials collected on a filter paper at the reactor exit or condensed on other reactor surfaces at the ambient temperature. Some of the tar was dissolved, immediately after weighing, in pyridine for molecular weight determinations. Gaseous products were collected outside the reactor in a trap, consisting of a tube packed with Porapak QS immersed in a dewer flask of liquid nitrogen (−196°C). Gaseous and condensible products were analyzed on a Perkin Elmer Sigma 2 gas chromatograph with dual flame ionization/thermal conductivity detectors. This system was connected to a Sigma 10 data station. Separate yields of CO, CO_2, CH_4, C_2H_6, C_2H_4, and H_2O, and yields of total C3's and total C4+ light hydrocarbons were measured.

Solvent extraction

Pyridine (MW 79.10, BP 115°C) is a strong solvent for bituminous coal and related materials. For example, 18-h Soxhlet extraction of the unpyrolyzed Pittsburgh No. 8 coal gave about 30% (as received) extract. Pyridine is also a good mobile phase in molecular weight determinations by size exclusion chromatography. An aliquot of the extract solution was removed for the molecular weight determination 2 hours after the start of extraction. Longer times resulted in changes in the extract molecular weight distribution that are believed to reflect secondary polymerization of extract in the boiling pyridine solution, rather than additional (preferential) extraction of higher molecular weight fractions. The extract yield was determined from the weight loss of the char after an additional 16 hours of extraction to promote efficient removal of pyridine soluble material.

Molecular weight determinations

Gel Permeation Chromatography (GPC) was employed for determining the MWD of tar and pyridine extract. GPC separates molecules in solution by molecular size. A Waters Associates ALC/GPC 201 GPC system with a UV absorbance detector was used. The separations were done on a set of 500 and 100 Å μ-stragel columns calibrated with tar samples, for which the molecular weight has been determined using vapor pressure osmometry (Oh, 1985). Two calibration methods (Yau et al., 1979) were employed. In the peak position method, the tar sample is fractionated into narrow molecular weight ranges and the MW of each fraction is related to the average retention volume of the GPC chromatogram. The other, the linear calibration method, has the advantage of not requiring fractionation of the sample since it assumes a log-linear relation between MW and column retention volume. Instead, it requires GPC chromatograms for two samples of known molecular weight.

Results

Yields of volatiles and extracts

Figures 1 and 2 show the yields of total volatiles (total weight loss) and tar (top) and of pyridine extract (bottom) as functions of peak pyrolysis temperature at 1 atm and at vacuum. Solid lines in Figures 1 and 2 are drawn to guide the trends in data. The large scatter is observed in vacuum pyrolysis data, probably due to poor heat transfer which results in large uncertainty in

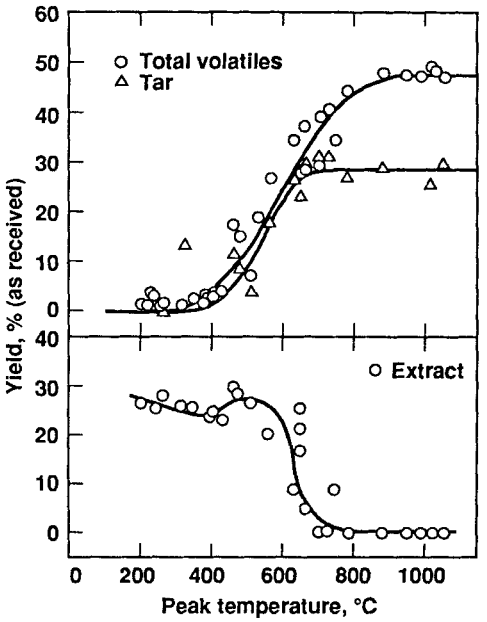

Figure 1. Yields of total volatiles, tar and pyridine extract from pyrolysis at 1 atm.

temperature measurements. Tar yields and total weight loss increase with peak temperature at both pressures, and both are higher at vacuum. These trends are in agreement with previous findings (Suuberg, 1977, 1978).

Extract yield initially decreases with increasing pyrolysis temperature, up to ~400°C, but as the coal starts to soften, the extract yield increases, exhibits a maximum at ~550°C, and then decreases strongly with further temperature increases. At temperatures between about 600 to 800°C, the decline in pyridine extract yields with increasing temperature appears to be somewhat stronger at 1 atm than at vacuum.

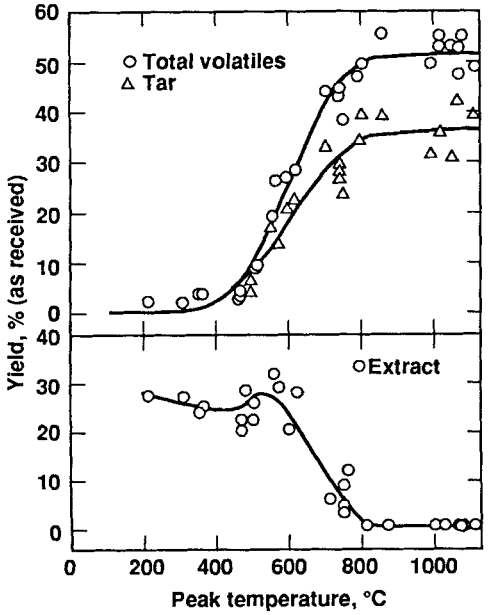

Figure 2. Yields of total volatiles, tar and pyridine extract from pyrolysis at vacuum.

These observations can be interpreted as follows. The initial decrease in the extract yield at low temperatures is due to partial conversion of the raw coal extractables to lower MW molecules (H_2O and CO_2) which evolve in the early phases of pyrolysis, and due to the absence of significant formation of additional extractables (metaplast). This interpretation is reflected in the model by two assumptions, that the evolution of light gaseous volatiles in the early stages of pyrolysis [gases (1) in the model] is due to decomposition of metaplast that existed in the raw coal, and that this decomposition is completed at low temperatures. As temperature increases into the softening regime, thermal cleavage of chemical bonds increases the extract yield, and tar evolution becomes measurable. At temperatures greater than 550°C, the metaplast formation reactions approach completion, the rate of tar transport becomes faster, and the pyridine extractables are also diminished by secondary cracking and repolymerization reactions within the coal particles. Therefore, rapid depletion of extractable materials is observed, and there is no extract yield at temperatures greater than about 700°C at 1 atm and about 800°C at vacuum.

Molecular weight distribution of pyridine extract and tar

Examples of the MWD of tar and extract from 1-atm pyrolysis at a peak temperature of 625°C and that of tar from vacuum pyrolysis at a peak temperature of 600°C are shown in Figure 3. The upper limit of the molecular weight of tar is about 1,200 while that of extract is about 1,500. However, the fraction of extract material having molecular weight greater than 1,200 is only a few percent of the total extract. Thus, to within a reasonable approximation, most of extract and tar have the same range of molecular weight, but tar has more of the lighter fractions and extract has more of the heavier fractions. These molecular weight data are consistent with our conceptualization of metaplast as unevaporated tar and support (but do not prove) our hypothesis that the yield of pyridine extract is a good estimate of the amount of metaplast remaining in the char.

Figures 4a and 4b show the number average molecular weight

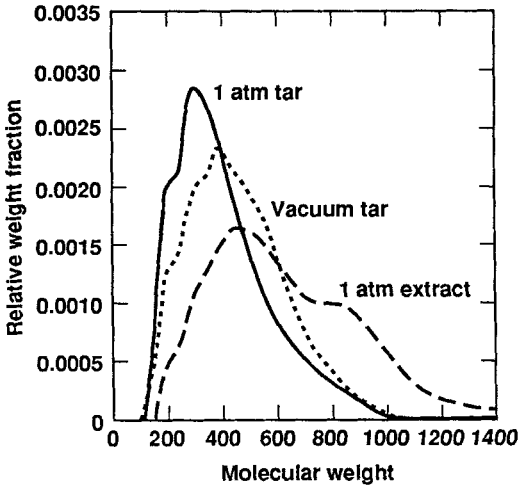

Figure 3. Normalized molecular weight distributions of 1-atm tar and extract (peak temperature = 626°C) and of vacuum tar (peak temperature = 600°C).

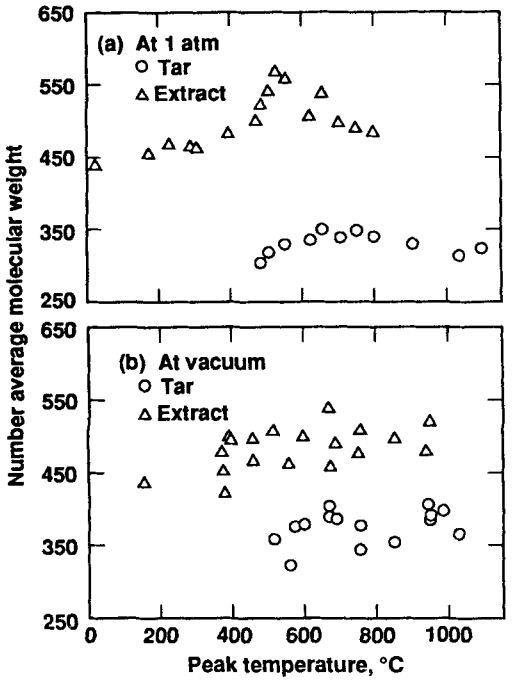

Figure 4. Number average molecular weights of tar and extract.

(MN) of tar and pyridine extract as a function of peak temperature (PT) at 1 atm and at vacuum. Since no tar is obtained at temperatures below 400°C and no extract at temperatures above 800°C at 1 atm and 950°C at vacuum, MN data for the two materials overlap in a comparatively narrow range of temperatures. The MN of 1-atm tar initially increases, stays about constant and then decreases slightly at PT ~800°C. The MN of vacuum tar may show a slight increase with increasing peak temperature, but the large scatter in these data precludes affirmation of a definitive trend. The 1-atm extract data display a maximum around 550°C while the MN of the vacuum extracts shows no significant change with increasing PT above 400°C.

The MN of vacuum tars are about 0.05 kg/mol higher than those of 1-atm tars. The heavy fraction which is missing in 1-atm tar but present in vacuum tar remains in the char at 1-atm pyrolysis and causes the extract to have a higher MN at around 550°C. At higher temperatures or longer holding times, this fraction is depleted by secondary reactions or mass transport. A higher MW for vacuum tar would also be predicted by pyrolysis models that acknowledge only external mass transfer limitations. For example, a tar evaporation model (Zacharias, 1979; Unger and Suuberg, 1981, 1983) would predict that heavier fractions of metaplast would be more readily transported at vacuum than at 1 atm. However, these correspondences do not establish the validity of neglecting internal transport, since an evaporation model by itself would predict that MN of 1-atm tars should increase monotonically with increasing PT, in contrast to observations (Fig. 4a).

Model Development

General description

Drawing on the work of Van Krevelen (1961) and Neavel (1982) and studies in this laboratory (Schaub et al., 1985a, b; Fong et al., 1985, 1986a, b), it was concluded that softening occurs when a critical temperature and concentration of a thermally-derived plasticizing agent, known as metaplast, are reached. Some metaplast is assumed to preexist in the coal as a bitumenlike material. As the coal is heated to a certain temperature, i.e., the softening point, the bitumens melt and the coal begins to soften. Further temperature increases result in chemical bond breaking which liberates additional metaplast that further augments plasticity. At higher temperatures or longer times, depletion of metaplast due to transport, decomposition, and polymerization causes the coal to resolidify. Thus the duration of the plastic stage reflects competition between metaplast generation and depletion processes which can, in general, involve both chemical and physical phenomena.

Once the coal develops fluidity, viscous flow closes off pores and the open pore structure disappears. The volatiles diffuse either to the particle surface or to bubbles dispersed throughout the molten coal. The characteristic time for lighter volatiles ($MW < 100$ amu) dissolved in the molten phase to diffuse to the surface of a 70 μm diameter particle is:

$$t_{c,s} \sim \frac{R_p^2}{D_{v,L}} \approx \frac{(35 \times 10^{-6}\ \text{m})^2}{10^{-11}\ \text{m}^2/\text{s}} \sim 100\ \text{s}.$$

The diffusivity value is lower than one used by Unger and Suuberg (1983), but it is more reasonable as will be explained later (Table 1). The characteristic time of order 100 s is too slow to explain experimentally observed pyrolysis rates (characteristic times of order 1 s or less at 600–800°C for 70 μm particles). However the characteristic time for the volatiles to diffuse into bubbles in the melt is ~0.1 s for a 1-μm radius bubble and less for smaller bubbles. Thus, light volatiles formed within the melt are much more likely to diffuse into bubbles rather than directly to the particle surface, and one can conclude that bubbles constitute a major vehicle for intra-particle transport of these volatiles. The growth of bubbles explains coal swelling during pyrolysis.

The maximum amount of the higher molecular weight (>1,000 amu) components of metaplast in bubbles is limited by their vapor pressure above the molten coal phase. Molecular diffusion through the melt and transport outside the particle may, therefore, be important for these species. Characteristic time for tar evaporation from 70 μm particle, estimated from the model by Unger and Suuberg (1981), at 1 atm and 600°C is 0.07 s for MW = 500 component and about 300 s for MW = 1,000 amu. The choice of vapor pressure model can significantly change the above characteristic time. For example, the model by Maiorella (1978) predicts much shorter characteristic times, 0.0004 s and 0.03 s for 500 and 1,000 amu components, respectively. Calculations by Oh (1985), using Maiorella's model, show that transport outside the particle may be rate-limiting for these heavier metaplast fractions at high pressures (~70 atm) and low temperatures (~400°C).

The present analysis assumes that the coal particles are spherical and isothermal, the latter being valid for small particles (~70 μm dia.) at a heating rate of 1,000°C/s (Oh, 1985). The spherical geometry is an approximation for coal particles in screen heater experiments, in which the geometry is between that of individual spheres and a thin slab. Spherical geometry was chosen because it is more general for a single particle model. Each particle is further assumed to have a spatially uniform

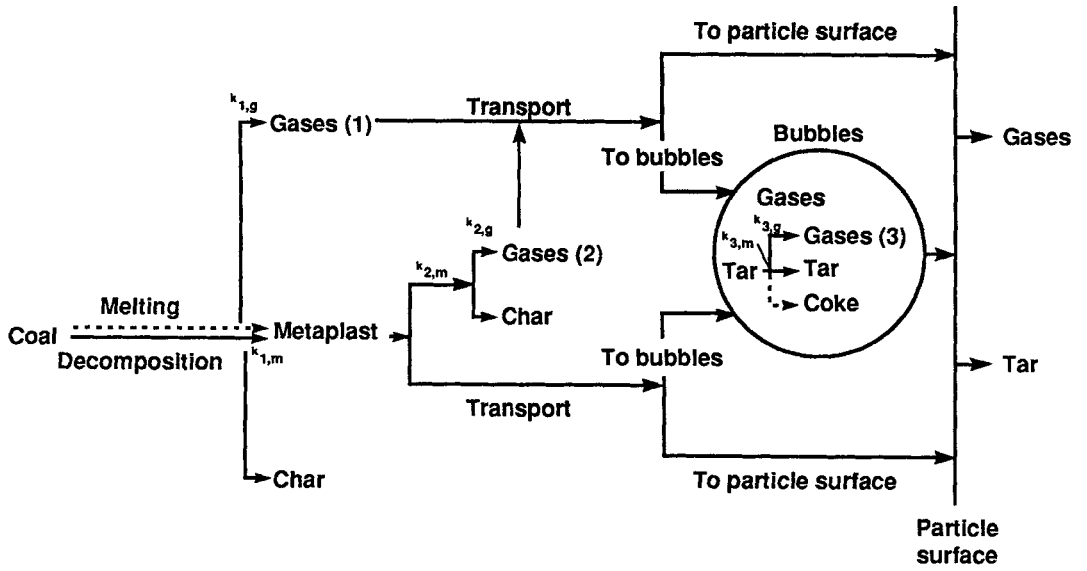

Figure 5. Chemical and transport rate processes contributing to volatiles evolution during pyrolysis of a softened coal particle.

bubble concentration, consistent with the isothermal assumption. Nonisothermal particles will have position dependent volatiles generation rate and, as a result, nonuniform bubble growth and escape rates which will create the gradient in bubble concentration. Any effects of compositional nonuniformities are neglected.

Essential physical and chemical features of the model are depicted schematically in Figure 5. Initial decomposition of coal generates gases, char and metaplast within the coal particles. Metaplast further decomposes and polymerizes to form more stable and more aromatic products as well as light gaseous volatiles. Physical melting of preexisting metaplast at the softening temperature is denoted by a dotted line. Since vaporized metaplast no longer functions as a plasticizing agent, metaplast vapor within bubbles and metaplast that escapes the particle are counted as tar.

Intra-particle volatiles transport is assumed to occur by diffusion of species dissolved in the coal melt and by expansion of bubbles. Bubbles are assumed to be generated at the onset of softening as deformation and flow of the molten coal transform interconnected pores into tiny sealed cavities of trapped gas. Bubbles may also be formed by spontaneous nucleation of gases or vapors that become saturated in the coal melt. Once bubbles are available, bubbles grow due to influx of volatiles from the melt. The surface of an expanding bubble is assumed to rupture upon reaching the particle surface, thereby releasing the bubble contents. Bubble movement due to buoyancy forces or to bulk motion of the melt is negligible because of the high viscosity of the molten coal. However, since the bubble distribution is assumed to always be spatially uniform throughout the particle, release of a bubble from the particle causes the remaining bubbles to be redistributed, and therefore, simulates a net movement of bubbles (and their cargo of volatiles) to the particle surface.

Chemical kinetics

The formation of gases (1) (Figure 5) and metaplast is modeled as unimolecular decompositions, first-order in the amount of the given material yet to be formed:

$$\frac{dV_i}{dt} = k_i(V_i^* - V_i) \tag{1}$$

where V_i and V_i^* are amounts of gases (1) or metaplast formed at time t and $t = \infty$, respectively. At $t = 0$, V_i for gases (1) is zero and V_i for metaplast is estimated as the yields of pyridine extractables from raw coal. Gases (1) originate from metaplast preexisting in the coal. Their formation is completed at a low temperature.

The depletion rates of metaplast in the liquid and of tar in the bubbles due to secondary reactions and, therefore, the formation rates of gases (2) and gases (3), respectively, are modeled as first-order in the amount of metaplast or tar locally available:

Rate of metaplast secondary reactions

$$\text{within molten coal} = k_{2,m}C_m \tag{2}$$

$$\text{within bubbles} = k_{3,m}B_m \tag{3}$$

$$\text{Rate of gases (2) formation} = \frac{dV_{g,2}}{dt} = f_{g,2}k_{2,m}C_m \tag{4}$$

$$\text{Rate of gases (3) formation} = \frac{dV_{g,3}}{dt} = f_{g,3}k_{3,m}B_m \tag{5}$$

where $f_{g,j}$, $j = 2$ or 3, is the fraction of metaplast converted to gases, and C_m and B_m are metaplast and tar concentrations in the liquid and bubble phases, respectively, expressed as kg metaplast/kg original coal.

The reaction rate constants, k, with appropriate subscripts, are expressed as $k_o \exp(E/RT)$ assuming a single-reaction model. A multiple-reaction model with distributed activation energies, which is used widely in coal pyrolysis studies (Howard, 1981), would better represent the cumulative reactivity of the range of bond strengths thermally labile in typical coal molecules than would a single-reaction model. However, the single-

reaction model is used here because its relative simplicity is advantageous when dealing with the combined complexity of kinetics and transport.

Conservation equations

Bubble Balance. The pores in solid coal are assumed to become bubbles in molten coal, and bubbles can also be generated by nucleation in the molten coal when the concentration of gases and vapors exceeds the saturation limit.

Bubble growth proceeds via the following mechanisms:

1. Addition of gas molecules by diffusion from the molten coal phase
2. Chemical reactions inside or at the surface of the bubble, including secondary reactions of tar vapor
3. Changes in gross physical forces such as internal or external pressure
4. Coalescence with other bubbles

Bubble coalescence is assumed to occur only by interfacial contact of two bubbles. The phenomenon of interbubble diffusion known to occur in foams is automatically accounted for in the treatment of net gas diffusion through the molten coal.

The growth and coalescence of bubbles are described mathematically as follows. Let n_j be the number of bubbles containing j molecules per unit mass of original coal. Then, the bubble conservation equations are

$$\frac{dn_j}{dt} = K_{j-1}n_{j-1}n_1 - K_jn_jn_1 + \frac{1}{2}\sum_{i=2}^{j-2} P_{i,j-i}n_in_{j-i} - \sum_{i=2}^{N} P_{i,j}n_in_j - E_{bj}n_j \quad (6)$$

for j from 2 to N, where K_j is the rate constant for volatiles diffusion through the molten phase to a bubble of size j; P_{ij} is the rate of coalescence of two bubbles containing i and j molecules, respectively; and E_{bj} is a term describing the rate of bubble escape at the particle surface.

The first two terms on the righthand side of Eq. 6 describe bubble growth and shrinkage due to diffusion of monomers, respectively. The quantity K_jn_1 gives the rate of monomers transport through the melt to or away from a bubble of size j when the concentration of monomers is expressed in terms of number of molecules/kg orig. coal. The corresponding rate of mass transport is therefore

$$K_jn_1 = \rho_o 4\pi a_j D_{v,L} Sh(n_1 - n_{eq}) \quad (7)$$

where

a_j = bubble radius
$D_{v,L}$ = molecular diffusivity of the volatiles in the liquid
Sh = Sherwood number based on bubble diameter
n_{eq} = equilbirium concentration of monomers in the molten coal phase at the interface between that phase and the bubble
ρ_o = density of the molten coal phase: assumed constant

For the present problem, the Sherwood number varies from 1 to 2 (Oh, 1985). However, the magnitude of the diffusivity varies by several orders of magnitude because of changes in coal viscosity, and, therefore, the small variation in Sherwood number is ignored.

Assuming an ideal solution of gases in molten coal, the equilibrium concentration (mol/m^3) of gaseous volatiles in the molten coal phase at the melt-bubble interface C^g_{eq} is determined by Henry's law, $C^g_{eq} = P_g/H$, while C^{mi}_{eq}, the corresponding quantity for metaplast is determined from Raoult's law, $C^{mi}_{eq} = \rho_L P_{t,i}/P_v$. The quantities P_g and $P_{t,i}$ are the partial pressure of gases and metaplast component i in the bubble phase, and P_v is the vapor pressure of pure metaplast component i, for $i = 1$ to N_{tar}, where N_{tar} is the total number of metaplast components of different molecular weight.

Bubble coalescence is assumed to occur via expansion and spatial contact of two adjacent bubbles. The corresponding coalescence rate constant, P_{ij}, is derived assuming that the centroids of spherical bubbles with radii a_i and a_j remain stationary because of high melt viscosity and surfaces expand radially with velocities of $\boldsymbol{a}_i$ and $\boldsymbol{a}_j$, respectively;

$$P_{ij} = \rho_o 4\pi(a_i + a_j)^2(|\boldsymbol{a}_i + \boldsymbol{a}_j|) \quad (8)$$

The rate of bubble expansion, $\boldsymbol{a}$, is affected by mechanical forces such as the internal and external pressures of the bubble, surface tension of the molten coal, and inertial and viscous forces, as well as by the rate of volatiles mass transfer into the bubble (Oh, 1985). It is dervied assuming the coal melt behaves as a Newtonian fluid of constant density, viscosity, and surface tension; liquid density $\gg$ gas density; and bubble radius $\ll$ distance between bubbles (Scriven, 1959; Barlow and Longlois, 1962). In a very viscous liquid like molten coal, the inertial terms are small compared to the viscous term and the bubble growth rate is

$$\frac{da}{dt} = \frac{a}{4\mu}\left(P_b - P - \frac{2\sigma}{a}\right) \quad (9)$$

where

P_b = total pressure within the bubble; sum of partial pressures of gaseous volatiles and tar vapor
P = ambient pressure; external pressure on the particle
μ = melt viscosity
σ = melt surface tension

Equation 9 is an approximation. For example, the coal may swell to an extreme extent and form a cenosphere. However, within the uncertainties in the knowledge of melt viscosity, the viscous force is the dominant term. The above simplified equation with a reliable description of melt viscosity provides a reasonable first approximation to the bubble growth rate.

It is assumed that all bubbles rupture upon contacting the particle surface, thereby releasing their inventory of volatiles outside the particle. The corresponding rate of bubble collisions with the particle surface is

$$\rho_o 4\pi(R_p - a_j)^2 \boldsymbol{a}_j n_j \quad (10)$$

The escape rate coefficient of bubbles sized j per kg original coal is then

$$E_{bj} = \frac{4\pi(R_p - a)^2}{\frac{4\pi}{3}R^3_{po}}\frac{da}{dt} \quad (11)$$

where R_p and R_{po} are the coal particle radius at time t and 0, respectively. Even though the mass is conserved, the number of molecules in bubbles may vary owing to secondary reactions of tar. However, for simplicity, this effect is omitted from the above bubble conservation equation.

Mass Balance for Gases and Metaplast. The material balances for both gases and metaplast in the molten phase include their rates of formation and of diffusion to bubbles and to the particle surface. Metaplast depletion by secondary reactions is also accounted for. Here, C_g and C_m are the average concentration of gas and metaplast in the melt, and $K_{j,g}$ and $K_{j,mi}$ are the rate constants (s^{-1}) for intra-melt diffusion of gases and metaplast component i. Assume that all gases have the same molecular weight and that the rates of formation and secondary reactions are the same for all metaplast components regardless of their molecular weight. The mass balance for gases is

$$\frac{dC_g}{dt} = k_{1,g}(V^*_{g,1} - V_{g,1}) + f_{g,2}k_{2,m}\sum_{i=1}^{N_{tar}} C_{m,i} - \sum_{j=2}^{N} K_{j,g}n_{1,g}n_j - E_gC_g \quad (12)$$

and the one for metaplast is

$$\frac{dC_{m,i}}{dt} = k_{1,m}(V^*_{m,1} - V_{m,1}) - k_{1,g}(V^*_{g,1} - V_{g,1}) - k_{2,m}C_{m,i} - \sum_{j=2}^{N} K_{j,m}n_{1,m}n_j - E_{m,i}C_{m,i} \quad (13)$$

for $i = 1, \ldots N_{tar}$. The rate coefficient of gaseous volatiles diffusion to the particle surface, E_g, is obtained from the steady-state material balance for gases dissolved in the coal melt by computing their steady-state radial flux at the particle surface (Oh, 1985; Oh et al., 1984):

$$E_g = \frac{3R_p^2}{R_{po}^3} D_{g,L}\sqrt{\frac{\sum_{j=1}^{N} K_j n_j}{D_{g,L}}} \quad (14)$$

The mass transfer rate of gases from the molten phase to the bubbles is relatively fast and the gas concentration in the molten phase is near its saturation level, which is small compared to the total amount of gases formed. A pseudosteady-state approach is therefore appropriate for deriving Eq. 14 (Oh et al., 1984).

The amount of metaplast transported to bubbles varies significantly with temperature. A steady-state analysis therefore is not always suitable for metaplast. Its rate of diffusion through the melt is derived assuming a parabolic concentration profile which satisfies the appropriate boundary conditions (Oh, 1985; Oh et al., 1984). Under this assumption, the flux of metaplast at the particle surface as a function of the spatially averaged metaplast concentration within the particle, $C_m(t)$, is

$$-D_{m,L}\frac{dC}{dr} = \frac{5D_{m,L}}{R_p}(C_m - C_s), \text{ at } r = R_p \quad (15)$$

where $C_s(t)$ is the concentration of metaplast in the melt phase at the particle surface. Since external mass transport of metaplast can be important for the case of low temperatures and higher pressures as noted earlier, both internal and extra-particle mass transfer resistances are included for each metaplast component. This feature allows the model to be applied to a wide range of molecular weights (up to at least 1,500 daltons), temperatures, and pressures. Under these conditions, it is found that the rate coefficient of transport from the particle surface for metaplast component i, $E_{m,i}$, is given by:

$$E_{m,i} = \frac{3R_p^2}{R_{po}^3}\frac{1}{\frac{1}{D_{m,g}}\frac{P}{P_{v,i}}\frac{\rho_L}{\rho_g} + \frac{1}{5D_{m,L}}} \quad (16)$$

The cumulative yields of gases and tar up to a time t' are obtained from E_g, E_m, and E_b:

$$\text{Gas Yield} = \int_0^{t'}\left(E_gC_g + \sum_{j=2}^{N} B_{g,j}E_{b,j}n_j\right)dt \quad (17)$$

$$\text{Tar Yield} = \int_0^{t'}\left(\sum_{i=1}^{N_{tar}} E_{m,i}C_{m,i} + \sum_{j=2}^{N}\sum_{i=1}^{N_{tar}} B_{m,i,j}E_{b,j}n_j\right)dt \quad (18)$$

$B_{g,j}$ and $B_{m,i,j}$ are, respectively, the mass of gases and tar component i in bubble size j. The extent of swelling is calculated from the number density of bubbles, bubble radii, and a mass balance for the condensed phase assuming it retains a constant density throughout the reaction period:

$$\frac{R_p}{R_{po}} = \left[\frac{\frac{4\pi}{3}\sum_{j=1}^{N} a_j^3 n_j + \frac{(C_m + \text{coal} + \text{char})}{\rho_o}}{\frac{4\pi}{3}R_{po}^3}\right]^{1/3} \quad (19)$$

Physical Properties. Data and correlations for physical properties needed to implement the model are summarized in Table 1.

The viscosity of the coal melt varies with temperature and the concentration of high MW, non-softened components (Schiller et al., 1977; Bockrath et al., 1977). We used two different viscosity-temperature correlations (Eqs. 20 and 21, in Table 1). In Eq. 21, the temperature dependence of the melt viscosity is treated only at low temperatures (<450°C) where alternate means of resolidification, namely metaplast depletion by repolymerization or transport, are negligible. Variations in the melt viscosity due to nonsoftened components are modeled using a correlation for densely packed suspensions (Frankel and Acrivos, 1967).

Coal plasticity data obtained from conventional or modified Gieseler plastometers give qualitative insights on how the coal viscosity varies with pyrolysis conditions. However, quantitative information directly applicable to the present model is not easily obtained from these instruments due to poorly defined flow fields, and due to heating rates and temperatures below those of current interest. Using a coal plastometer specifically designed to overcome these limitations, Fong et al. (1985, 1986a, b) measured a minimum viscosity of order 10^3 Pa · s for molten Pittsburgh Seam bituminous coal at heating rates of several hundred °C/s and peak temperatures exceeding 500°C. The constants in Eqs. 20 and 21 were chosen so that both correlations give a minimum viscosity value of this order of magnitude.

The linear temperature dependence for modeling volatiles dif-

Table 1. Correlations for Physical Properties*

*Melt Viscosity [Pa · s]***:

$$\mu = \frac{1 \times 10^{-11} \exp(45{,}000/RT)}{(1-\phi)^{-1/3} - 1.0} \tag{20}$$

$$\mu = \frac{1 \times 10^{-8} \exp(45{,}000/RT')}{(1-\phi)^{-1/3} - 1.0} \tag{21}$$

where

ϕ = wt. fraction of metaplast
$T' = T$ at temperatures < 723 K
$T' = 723$ K at temperatures > 723 K

Diffusivity of Volatiles in Molten Coal [m^2/s]:

$$D_v = \frac{1 \times 10^{-11}\, T}{\mu^q} \tag{22}$$

where

$q = 0.5$ for gases and 2/3 for metaplast

Vapor Pressure of Metaplast [atm]:
Maiorella's Model***:

$$P_v = 6.23 \times 10^5 \exp(-561\ \mathrm{MW}^{0.474}/T) \tag{23}$$

Unger and Suuberg's Model†:

$$P_v = 5.74 \times 10^3 \exp(-255\ \mathrm{MW}^{0.576}/T) \tag{24}$$

Surface Tension‡: 0.03 N/m
Solubility of Gas in Molten Coal [atm $(mol/m^3)^{-1}$]:

$$H = \frac{2.792 \times 10^7 \exp(314/T)}{\rho_L} \tag{25}$$

where

ρ_L = molar density of molten phase

Molecular Weight Distribution of Metaplast at Formation, Figure 7:

Macropore Volume§: 4×10^{-5} m^3/kg coal

*Unless otherwise noted, the correlations are developed by Oh (1985).
**Frankel and Acrivos (1967), and Oh (1985).
***Maiorella (1978).
†Unger and Suuberg (1983).
‡Attar (1978).
§Gan et al. (1972).

fusivity in molten coal (Eq. 22) is taken from several theoretical correlations for gas diffusivities in liquids such as those by Arnold, Wilke and Chang, and Akgerman and Gainer (discussed in Reid et al., 1979). The exponent on viscosity is assumed to be 0.5 for gaseous volatiles and 2/3 for metaplast of all molecular weight based on several experimental studies (Reid et al., 1979). A typical diffusivity of a gaseous solute in a hydrocarbon liquid at room temperatures is around 1×10^{-9} m^2/s when the viscosity is on the order of 1×10^{-3} Pa · s. Since the minimum viscosity of the coal melt of interest is approximately 10^3 Pa · s at temperatures around 500°C, the constant in Eq. 22 is adjusted to give a maximum diffusivity of 1×10^{-11} m^2/s.

The surface tension of molten coal is understood poorly, but probably varies with temperature, pressure, and viscosity. For example, experimental data on coal liquids show that the surface tension, in general, decreases with increasing temperature and pressure, but the magnitude of the decrease is small compared to that of the viscosity or the diffusivity (Hwang et al., 1982). In addition, an empirical correlation of surface tension with viscosity for pure liquids (Pelofsky, 1966) suggests a constant surface tension throughout the region of high viscosities. In the present analysis, the surface tension of coal melt is assumed to be a constant.

The solubilities of gases in the molten coal are estimated using H_2, CH_4, and CO_2 solubilities in various hydrocarbon liquids. The vapor pressure of metaplast could be estimated from vapor pressure correlations for organic liquids, based on critical properties (Grey and Wilson model, Wilson et al., 1981; Grey et al., 1983) or from structural information for the tar vapor (Edwards et al., 1981). However, both estimation methods are complicated. The former requires information on the molecular weight and specific gravity (SG) of tar components. The latter

requires knowledge of the vapor pressure of each component at one temperature and rather detailed information on tar molecular structure, and is limited to molecular weight <475 daltons. An alternative, used here, is a more simple, semiempirical model based on the Clausius-Clapyron equation and the assumption that the latent heat of vaporization of a given component is linearly proportional to its molecular weight. Thus, one needs the molecular weight of each component and the vapor pressure of any one component at two temperatures. Such a correlation applicable to coal tar and metaplast was proposed by Homann (1977). Modifications were later given by Maiorella (1978), Eq. 23, and by Unger and Suuberg (1983), Eq. 24, by correlating vapor pressure of selected model compounds with molecular weight.

Figure 6 compares vapor pressures predicted from these two semiempirical models at 1,000°C as a function of MW, with corresponding predictions from the Grey and Wilson model, which was derived from vapor pressure data for coal liquids of molecular weight up to approximately 350 daltons. Although the Grey and Wilson measurements covered a more narrow MW range than that of current interest, they were still useful in assessing the validity of the two semiempirical correlations. Figure 6 shows that, above 300 daltons, Maiorella's correlation predicts much higher vapor pressures than other correlations. Unger and Suuberg's correlation gives too low a vapor pressure for the present model to predict the observed tar yield at temperatures between 450–600°C, while use of Maiorella's model at high temperatures overestimates metaplast vapor pressure and causes the model to overpredict tar yield (Oh, 1985). Both viscosity correlations (Eqs. 20 and 21) and vapor pressure correlations (Eqs. 23 and 24) were employed in deriving kinetic parameters for tar and gas evolution by fitting the model to laboratory pyrolysis data.

The MWD of metaplast employed in the present vapor pressure calculations is shown in Figure 7. This distribution was calculated from Oh's (1985) measurements of the MWD's of tar and the pyridine extract of char from low temperature pyrolysis of Pittsburgh No. 8 coal. Since the formation rate of each metaplast MW fraction is assumed to be the same, the MWD of metaplast generated due to decomposition of coal stays constant regardless of the formation temperature.

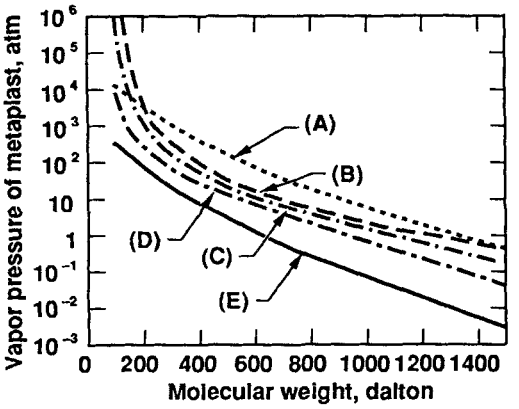

Figure 6. Comparison of vapor pressure predictions of metaplast at 1,000°C.

(A) Maiorella; (B) Grey and Wilson, SG = 900 kg/m^3; (C) Grey and Wilson, SG = 1,000 kg/m^3; (D) Grey and Wilson, SG = 1,200 kg/m^3; (E) Unger and Suuberg.

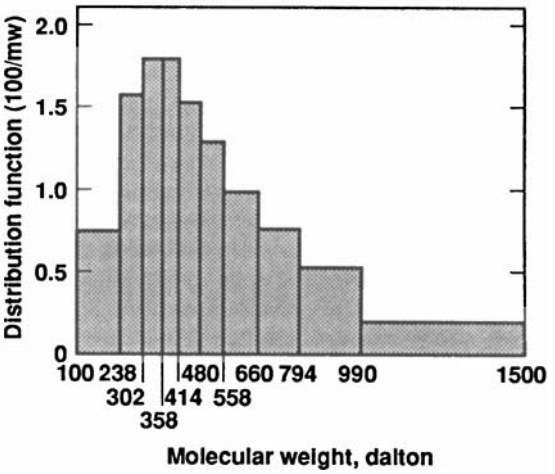

Figure 7. Molecular weight distribution of metaplast at formation.

Model Predictions and Discussion

Model simplification

Inclusion of the coagulation contributions to bubble growth (terms 3 and 4 on the RHS of Eq. 6) created significant numerical complications. Thus, in implementing the model, bubbles were assumed to grow solely by diffusive influx of volatiles. Even without coagulation, prediction of the time-dependent bubble size distribution remains difficult because bubbles of different size have different growth rates, which are determined by solving Eqs. 7 and 9 simultaneously. Sectional representation, a numerical technique developed by Gelbard et al. (1980) for computing particle size distributions in aerosol dynamics, was employed. The method is based on dividing the bubble size domain into m arbitrary sections and assigning one integral quantity, such as mass v, to each section. This technique has the advantages of reducing the number of equations and of conserving the integral quantity within the computational domain. The dimensionless domain w, where $w = \ln (v/v_{min})/\ln (v_{max}/v_{min})$, is divided into 20 equal-size sections. The bubble growth rates, dw/dt and $d\gamma/dt$ where $\gamma = \ln (a/a_{min})/\ln (a_{max}/a_{min})$, are solved at section boundaries along with the 20 sectional bubble mass balances and the volatiles balance in the melt. The growth rates of bubbles within a section are estimated by linear interpolation of the growth rates at the section boundaries.

Figure 8 plots the changes in the bubble size distribution at various times and shows that the growth of bubbles shifts the bubble size distribution to the larger bubble sizes and that the rapid growth of smaller bubbles promptly leads to a large fraction of the volatiles mass being in bubbles near the minimum size. Thus, the model predicts that while, throughout pyrolysis, there may be a few bubbles in every size range considered, most of the bubbles grow into practically one size and essentially all the mass transported from the melt to bubbles enters those bubbles with the smallest stable size. This important result greatly

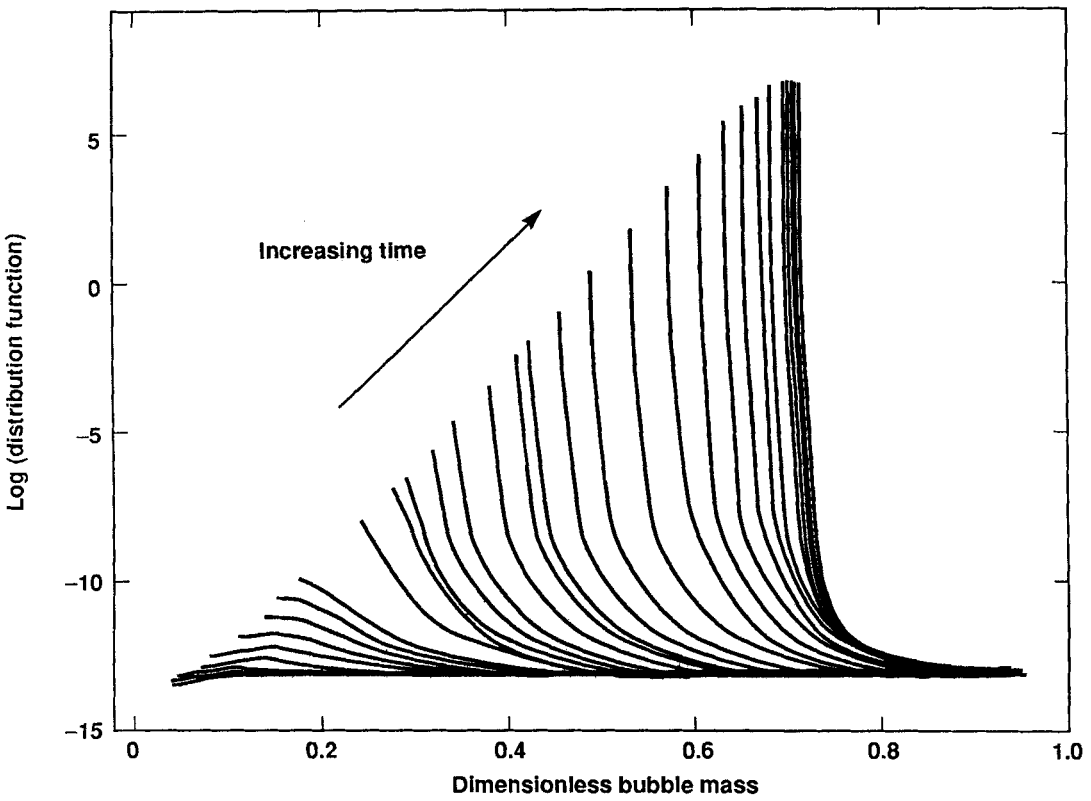

Figure 8. Time-dependent variations in bubble size distribution.
Dimensionless bubble mass = $\ln (v/v_{min})/\ln (v_{max}/v_{min})$ where v is the mass of a bubble

simplifies the governing equation of bubble growth, permitting the approximation of uniform bubble sizes.

Initial generation of bubbles

Little is understood about bubble genesis in the freshly formed coal melt including the phenomena governing their initial size and generation rate. Quantitative modeling of bubble initiation as a function of pyrolysis conditions is difficult to formulate. The present model treats pores in the solid coal as one source of bubbles. Coals have significant pore volume with porosities varying from 2.5 to 18% and pores which have openings ranging from 4–5 Å to around several microns. Changes in the pore structure of softening coals with heating have been studied extensively, primarily under carbonization conditions. Results show that both micro- and macro-pore volumes reach maxima at a certain temperature (Franklin, 1949; Toda, 1970; Muira et al., 1980; Singla et a., 1982).

Coals have a significant fraction of fine pores, the configuration of which is related to the way coal micelles are bound together (Franklin, 1949; Hirsh, 1954). However, calculations show that the survival of submicron pores into the plastic period is questionable because they are very likely to dissolve in the molten phase. The existence of fine pores in chars from pyrolysis of softening coals implies that fine pores reappear as the coal resolidifies and contracts. It is assumed that bubbles which survive the initial softening of the coal originate from macropores and that the initial number of density of these bubbles can be calculated from the macropore volume of the coal given a reasonable approximation for the minimum bubble size which is stable in the newly formed coal melt.

Another possible mechanism for bubble initiation is spontaneous nucleation. Application of nucleation rate theory to predict the bubble generation rate is considered to be unjustified, since it involves great uncertainties in the rate function of a highly nonhomogeneous medium such as molten coal. Instead, calculations were made to test whether nucleation of bubbles could be a rate-limiting step in the transport processes for the pryolysis conditions of interest (Oh, 1985). It was concluded that, in light of the uncertainties in present knowledge of the solubilities of volatiles in the molten coal, nucleation of bubbles is not a rate-limiting process. This contrasts with an earlier conclusion by Attar (1978) who apparently underpredicted bubble nucleation rates by underestimating pyrolysis gas generation rates from inappropriate kinetic data. Thus, one can assume that bubbles, nucleated or derived from the pores, exist in the molten coal at the onset of softening. The number density of bubbles then decreases as bubbles grow and are released from the particle.

Derivation of kinetics parameters

Table 2 summarizes kinetic parameters inputted to the model from other sources. Since gases (1) are assumed to be formed at low temperatures (<400°C) from preexisting metaplast, their corresponding kinetic parameters ($k_{o1,g}$, $E_{1,g}$, and V_g^*, in Eq. 1) are obtained by fitting total volatiles yields from 1-atm, vacuum pyrolysis at peak temperatures below 400°C to a single reaction model, without considering transport.

The parameters for tar cracking reactions in bubbles and for formation of gases (3) (Eqs. 3 and 5) are obtained from the work of Serio (1984, 1987).

Table 2. Kinetic Parameters Inputted to the Model from Other Sources

Gases (1) Formation Reaction:*

$V^*_{g,1}$	0.0285 kg/kg orig. coal
$E_{1,g}$	112 kJ/kg mol
$k_{o1,g}$	1×10^{13} 1/s

*Metaplast Formation Reaction**:*

V^*_m	0.7 kg/kg orig. coal

Tar Cracking Reaction in Bubbles†:

$E_{3,m}$	64.5 kJ/kg mol
$k_{o3,m}$	9.96×10^2 1/s
$f_{g,3}$	1.0

*Obtained from pyrolysis data at low peak temperatures. The $k_{o1,g}$ is a fixed parameter. **Fong (1986a,b). †Serio (1984).

The Arrhenius kinetic parameters for metaplast formation and decomposition reactions and for formation of gases (2) ($E_{1,m}$, $k_{o1,m}$, $E_{2,m}$, $k_{o2,m}$, and $f_{g,2}$ in Eqs. 1, 2 and 4) were determined from the complete transport model and the pryolysis data at peak temperatures above 400°C at 1 atm. The ultimate amount of metaplast that can be formed, V^*_m, was assumed to be constant. For the present coal, the value $V^*_m = 0.7$ kg/kg original coal was used, based on the work of Fong et al. (1986a, b), who found that the maximum yield of pyridine extract plus volatiles was between 0.65 and 0.76 (as received) when this coal was pyrolyzed in a screen heater reactor at low temperatures and then rapidly quenched with liquid nitrogen.

The initial number density of bubbles is also left as a fitted parameter. Essentially all the gas formed is transferred to bubbles because the equilibrium-allowed amount of dissolved gases in the melt is small. As a result, increasing the bubble number density at a fixed rate of pyrolysis gas generation means that a smaller amount of gaseous volatiles is transported to each bubble. This reduces the bubble growth rate, which lowers the volatiles yield and increases the particle swelling. However, the amount of tar in each bubble does not depend on the bubble number density but rather on its vapor pressure, except at high temperatures where all metaplast is vaporized. Thus, the total amount of tar in bubbles increases with bubble number density, and one can observe more secondary reactions of tar in bubbles at a higher bubble number density. In the calculation of kinetic parameters, a high bubble number density results in rapid metaplast formation and slow liquid-phase decomposition reactions, while a low number density gives slow metaplast formation rate and fast liquid-phase secondary reactions at high temperatures. Current understanding precludes *a priori* predictions of the initial number density of bubbles in the coal melt for different pyrolysis conditions, so this quantity is determined as a fitted parameter as mentioned above. As discussed before, bubbles which survive through softening probably originate from macropores. Thus, the initial number density of bubbles can be estimated by assuming a fixed pore volume and changing the pore radius (a_{pore}) within the range of the macropore sizes. The volume of macropores in bituminous coals varies from 1.5×10^{-5} to 4×10^{-5} m^3/kg (Gan et al., 1972). The pore volume in this work was fixed at 4×10^{-5} m^3/kg.

The requirement of six fitted parameters may seem excessive. However, the model utilizes three independent sets of laboratory data to obtain these parameters: total gas yield, tar yield, and extract yield. This corresponds to deriving two fitted parameters per data set, rather than three per data set usually obtained when fitting data on pyrolysis weight loss or product yields to a single reaction model.

To examine the effect of two different viscosity-temperature correlations and two vapor pressures correlations on model performance, three different combinations of viscosity and vapor pressure correlations (Cases A to C, Table 3) were considered, and the influence of each combination on model predictions was studied. Table 4 summarizes three sets of six best-fit parameters obtained by using the model with each of the above cases.

Model predictions of transient product distribution, plasticity and swelling

The kinetics parameters for Case A were used in this calculation. The product distribution as a function of total heating time predicted for pyrolysis at 1 atm is shown in Figure 9a for a heating rate, peak temperature, and holding time of 448°C/s, 760°C, and 5 s, respectively. At around 400°C, the coal starts to soften (predicted viscosity = 4×10^4 Pa · s); and essentially all of the gas formed is immediately transported into bubbles, because the equilibrium-allowed amount of dissolved gases in the melt is small compared to the amount of pyrolysis gas being formed and because the rate of gas being transported into bubbles is fast. In contrast to the gaseous volatiles, the tar content in bubbles is limited by its vapor pressure. The transport of metaplast across the melt-bubble interface is sufficiently fast to justify the assumption that tar vapor in bubbles is in equilibrium with the molten phase. As temperature increases, Maiorella's vapor pressure correlation predicts that the equilibrium-allowed concentration of tar in bubbles will increase rapidly. Simultaneously, the yields of gases and tar evolved from the coal increase rapidly. For the above temperature-time history, the metaplast formation reactions attain 99% of completion before the peak temperature is reached. By the time the peak temperature is attained, the low residual concentration of metaplast results in a high melt viscosity, which in turn inhibits bubble growth and tar removal from the particle. Thus, most of the tar remaining in the bubbles is decomposed to gases, resulting in a large gas hold-up in bubbles at longer pyrolysis times.

As the metaplast formation reactions approach completion, the coal starts to resolidify and transport by bubble growth becomes less important. Some of the gases in bubbles may dissolve back into the molten phase and gas release occurs by diffusion of dissolved gases through the melt. Even though the model allows for this mode of volatiles transport to the particle surface, their rate of diffusion through the melt is extremely slow. Thus, almost all gases formed at this stage of pyrolysis are trapped in bubbles. Once sufficiently connected porosity is reestablished by resolidification of the melt, these volatiles are transported to the particle surface by diffusion and hydrodynamic flow through pores. Since the present model does not treat volatiles transport through pores, any gas trapped in bubbles upon resolidification is assumed eventually to diffuse out of the particle after the resolidification. Metaplast remaining in the particle is either consumed in secondary reactions, if there is sufficient residence time at high temperatures or is retained as liquid within the particle as the coal cools down.

The predicted variations in viscosity and the swelling ratio are

Table 3. Physical Property Cases Studied with the Model

Case	Vapor Pressure Correlation		Temp. Dependence in Viscosity Model	
	Maiorella*	Unger and Suuberg**	Abbr. Temp. Range†	Full Temp. Range‡
A	X		X	
B		X	X	
C	X			X

*Eq. 23, Table 1. †Eq. 20, Table 1.
**Eq. 24, Table 1. ‡Eq. 21, Table 1.

shown in Figure 9b. After a rapid initial decline at about 0.8 s the melt viscosity starts to increase at around 1.5 s, and the molten coal starts to resolidify. The predicted "plastic" period, i.e., where the melt viscosity is less than 2×10^4 Pa · s, is about 0.6 s, which is much shorter than the 0.9 s of plastic period measured under similar conditions by Fong et al. (1985, 1986a) as shown in Figure 10. With parameters employed, the model predicts that metaplast depletion in the melt arises from rapid transport to bubbles rather than from secondary reactions. The shorter predicted plastic period thus implies that the metaplast vapor pressure is overestimated by Eq. 23 at temperatures higher than 600°C.

Since the swelling is a result of bubble growth and plasticity, the rapid build-up of bubble volume during the plastic period causes the swelling ratio (R_p/R_{po}) to increase. However, after the peak temperature is reached, the high melt viscosity inhibits further bubble growth and release. Therefore, the swelling ratio stays constant at 4.2 even though the bubble pressure is increasing due to higher gas concentration.

The effect of the rate of the tar secondary reactions in bubbles on the extent of swelling and other pyrolysis behavior may not be as important as the impact of metaplast vapor pressure. Figure 9 shows that the rate of tar conversion to gases, predicted by a single reaction model, is slow during heat-up and that most of the gases (3) are formed after the coal starts to resolidify. If the secondary reactions of tar in bubbles occur rather rapidly during the plastic stage, the enhanced growth due to the resulting gas formation causes more bubbles to be released from the particle, thus lowering both the number density of bubbles and the amount of gas hold-up. Serio et al. (1983, 1987) found that data on homogeneous (vapor phase) cracking reactions of freshly formed coal pyrolysis tar were well correlated by a kinetic model based on three independent parallel reactions, involving distinct tar lumps of high, medium and low reactivity. The rate of tar cracking, predicted by their three-lump model is somewhat faster than corresponding predictions from the present single reaction model. On the other hand, the Serio et al. model predict a lower overall contribution of intra-bubble tar cracking to net gas production, since their three-lump model requires about 40 wt. % of the tar vapor to remain unreactive under the present pyrolysis conditions. Therefore, the three-lump model may lower and thus improve the swelling predictions.

Model predictions of yields of tar, metaplast and total volatiles

Figures 11a through 11c compare the model predictions of total volatiles yields, tar yields, and the amount of metaplast remaining in the particle for the three cases in Table 3 to the corresponding experimental data from 1-atm pyrolysis. Unless stated otherwise, the time-temperature history employed in the calculations was linear heat-up at 1,000°C/s, followed immediately by natural cooling. The temperature-time history for the cooling period, Eq. 27, was derived assuming radiative and convective cooling of the screen; and the constants b_1 and b_2 were obtained by fitting Eq. 27 to measured temperature-time histories (Oh, 1985):

$$T = H_r t + T_o, \quad t \le t_p \tag{26}$$

$$T = \left[\frac{\frac{b_2}{b_1}}{\left[1 + \frac{b_2}{b_1 T_p^3}\right] \exp\left[3 b_2 (t - t_p)\right] - 1} \right]^{1/3} \quad t > t_p \tag{27}$$

where T_p and H_r are the peak temperature and the heating rate, 1,000°C/s; $t_p = (T_p - T_o)/H_r$; $b_1 = 2.20 \times 10^{-10}\ \mathrm{K^{-3} \cdot s^{-1}}$; and $b_2 = 6.73 \times 10^{-2}\ \mathrm{s^{-1}}$.

The model predictions of total volatiles and of tar obtained using Maiorella's vapor pressure model and a restricted temperature dependence for melt viscosity (Case A) are in the best overall agreement with experiment for the three cases considered in Table 3. However, the correlation by Maiorella gives

Table 4. Effect of Vapor Pressure and Viscosity Correlation on Kinetic Parameters*

	Case A	Case B	Case C
$E_{1,m}$, kJ/kg · mol	90.9	67.4	183.
$k_{o1,m}$, 1/s	2.88×10^6	3.20×10^4	1×10^{13}
$E_{2,m}$, kJ/kg · mol	78.7	70.8	108.
$k_{o2,m}$, 1/s	2.98×10^5	2.96×10^4	3.48×10^7
$f_{g,2}$	0.053	0.284	0.205
a_{pore}, μm	0.076	0.080	0.094

*From two vapor pressure models and two viscosity models.

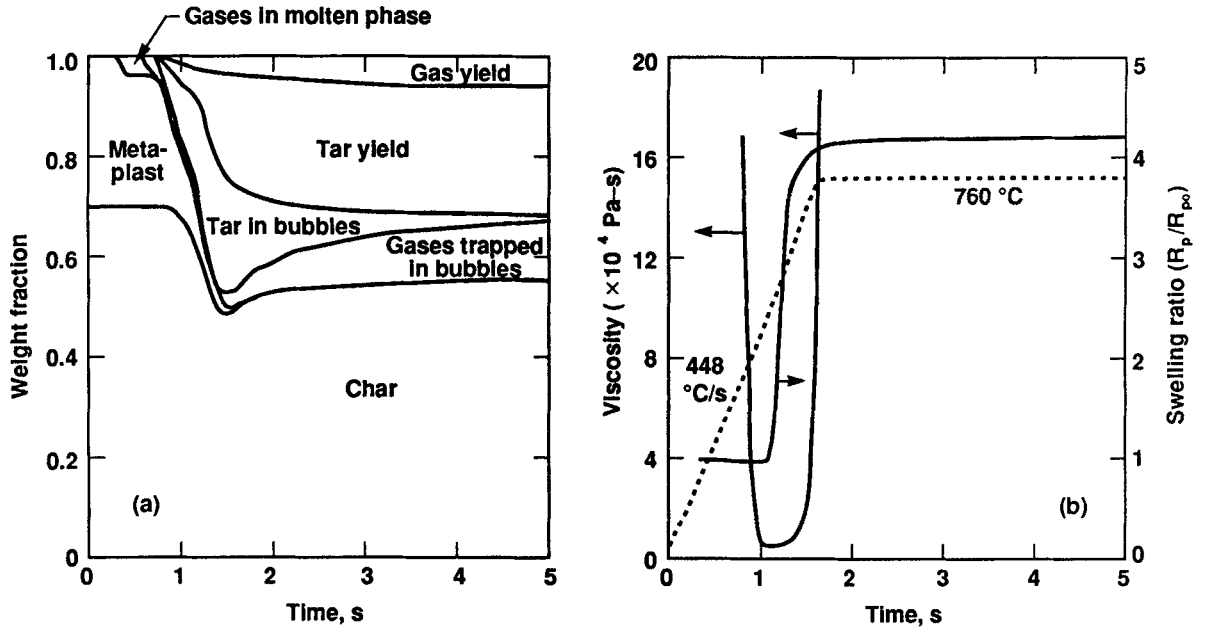

Figure 9. Predicted product distribution (a) and variations of viscosity of coal melt and swelling ratio (b) during coal pyrolysis at 1 atm.

Heating rate = 448°C/s; holding temperature = 760°C ---, temperature-time history

higher metaplast vapor pressures at all temperatures, so the model predicts more extensive metaplast evaporation into bubbles, resulting in a low melt concentration of metaplast and premature resolidification of the molten coal. Furthermore, since most of the secondary gases are formed by tar cracking in bubbles, this case causes the model to predict that a large fraction of the secondary gases end up trapped in bubbles (~7 wt. % at a peak temperature of 1,000°C).

The correlation by Unger and Suuberg (1983) does not give a sufficiently high vapor pressure to predict the tar yields at low temperatures. As a result, the model predictions of integral yields of pyrolysis products at different peak temperatures do not fit the data as well as Case A. However, at higher temperatures, use of the Unger and Suuberg correlation gives somewhat better model predictions of observed tar (Figure 11b) and metaplast (Figure 11c) yields, implying that the actual vapor pressures may be lower than those predicted by the Maiorella model under these conditions. This would also mean that liquid-phase secondary reactions would have a more significant role in secondary gas formation and in supplementing transport as a means of metaplast depletion. Thus, the form and temperature dependence of the vapor pressure correlation strongly affect how the model partitions metaplast and tar between the bubble and the molten coal phases as well as what contributions from secondary reactions the model assigns to each of these phases.

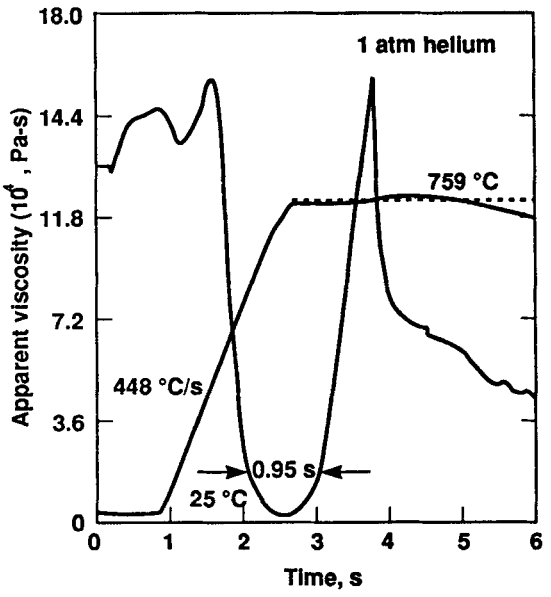

Figure 10. Measured apparent viscosity of Pittsburgh seam No. 8 bituminous coal under rapid heating during 1-atm pyrolysis (Fong, 1986a).

With the viscosity correlation showing a full-range temperature dependence (Case C), the model predictions of both tar and total volatiles yields are in poorer agreement with the data (Figures 11a and b) than the corresponding results using an abbreviated temperature effect on viscosity (Case A). This finding is consistent with the changes in melt viscosity with time and temperature calculated by each correlation. Examples of the melt viscosities predicted by the model for all three cases at a heating rate of 448°C/s and a peak temperature of 760°C are shown as a function of time in Figure 12. Again, this particular time-temperature history was chosen to compare the model predictions with measured values of an apparent viscosity shown in Figure 10. The viscosity predictions for Case C show a sharp minimum at 1.27 s, and the plastic period is much shorter than those for the other two cases. The attendant higher melt viscosities at both low and high temperatures inhibit the growth of bubbles and, therefore, the model generally predicts lower volatiles and tar yields for Case C than for Case A.

A longer plastic period and slightly slower rate of molten coal resolidification are predicted by using a correlation that gives

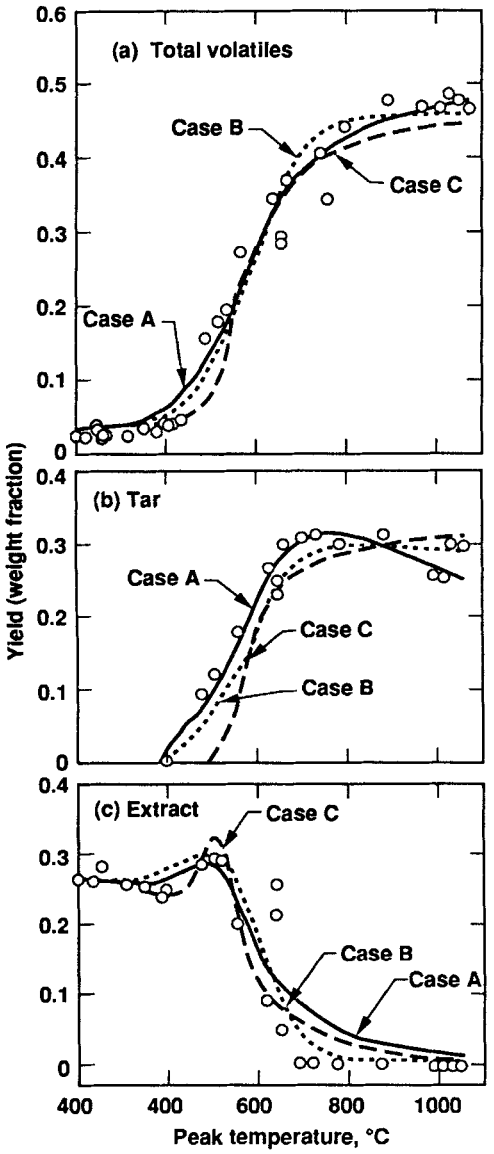

Figure 11. Yields of total volatiles, tar, and pyridine extract from 1-atm pyrolysis with model predictions.

Model predictions are for the three cases in Tables 3 and 4.

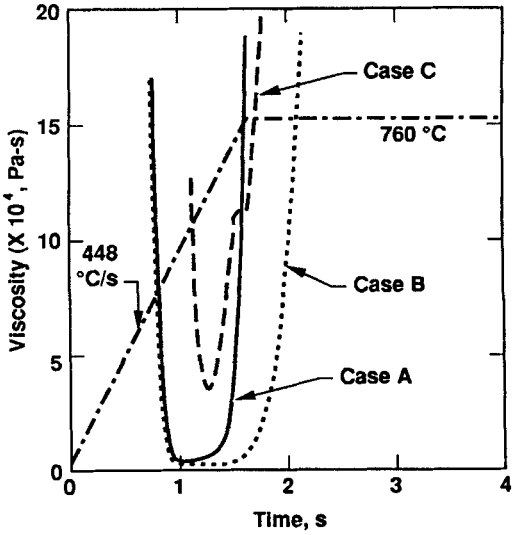

Figure 12. Predicted variations of viscosity of coal melt at 1 atm, as coal is heated to 760°C at 448°C/s and held at that temperature.

Kinetic parameters in Table 4, Case B, were used.

lower metaplast vapor pressures (Case B vs. Case A, Table 3). This is expected since Case B favors more retention of metaplast within the liquid phase. Similarly, Case A predicts that resolidification of the coal occurs sooner (Figure 12), because of greater evaporative loss of metaplast to bubbles. Consequently, the predicted plastic period is shorter than the measured value. The predictions of viscosity with Unger and Suuberg's vapor pressure model agree quite well with the measured viscosity. From this observation and the above effects of Case A vs. Case B on product yields, one can conclude that the true metaplast vapor pressure for this coal is more reasonably estimated by Maiorella's model at lower temperatures (≤600°C) and by Unger and Suuberg's model at higher temperatures.

It is encouraging that the correlation of temperature effects on melt viscosity, which gives better predictions of experimentally determined apparent viscosities of softened coal (Cases A and B), also gives better predictions of tar, metaplast and total volatiles yields.

The model predictions of the extent of swelling range between 4 and 4.4 for all three cases (Oh, 1985) which is roughly two to three times higher than expected. Observed swelling ratios of a single particle were found to range between 0.9 and 4, but mostly at around 2 (Essenhigh and York, 1965; Sung, 1978; Matsugna, 1978; Dolan, 1980; Lowenthal et al., 1986; Tsai and Scaroni, 1987).

Model predictions of pressure, particle size and heating rate effects

Pressure Effects. It is well known that softening coals show stronger effects of total external pressure on volatiles yield than nonsoftening coals (Howard, 1981). For example, Suuberg et al. (1978, 1979) and this work found that volatiles yield decreases with increasing pressure in bituminous coal pyrolysis, with most of the effect being a consequence of reduced tar yield. Volatiles and tar yields predicted by the present model at three different pressures are plotted as a function of peak temperature in Figure 13. Unger and Suuberg's vapor pressure model, Eq. 24, and the kinetic parameters listed in Table 4 (Case B) were used.

An increase in external pressure on the particle means that the bubble pressure must be increased correspondingly to sustain a given growth rate since more work is required for bubble expansion. Similarly, for a given internal volatiles generation rate, the bubble growth rate will decrease with increasing external pressure. Simultaneously, the mole fraction of tar in bubbles declines because the partial pressure of tar in bubbles rises only modestly with pressure due to the Poynting vapor pressure correction. Thus, the amount of metaplast transported by bubbles for a given mass of gas cotransferred decreases, and observed tar yield decreases.

The predicted tar yields at vacuum are somewhat higher than the measured values at peak temperatures between 500 and 700°C, as shown in Figure 14. The calculated tar yields at 69

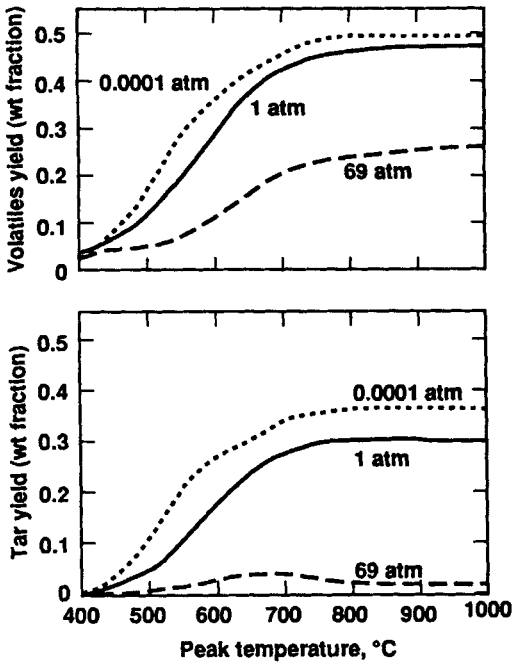

Figure 13. Model predictions of the pressure effect on total volatiles and tar yields. Calculations made for pyrolysis of softening coal heated to different peak temperatures.

atm (Figure 13) are significantly lower than the experimental data (Suuberg, 1978). Thus, while the present model properly predicts the major qualitative trends in observed effects of pressure on pyrolysis yields, quantitative calculations of pressure effects require further analysis and model refinements. One such refinement is to model the effect of total pressure on the initial number density of bubbles, such as a lower initial number density at higher pressures. This modification will help overcome the inability of the current model to properly simulate

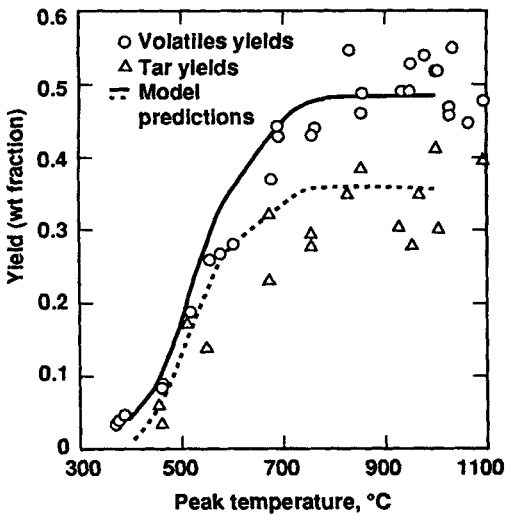

Figure 14. Comparison of tar and total volatiles from vacuum pyrolysis with model predictions.
Parameters from Table 4, Case B, were used for model predictions.

effects of pressure on plasticity and may improve the model predictions of volatiles yields at different pressures.

The predicted final swelling ratios (R_p/R_{po}) at different peak temperatures and at three pressures are shown in Figure 15. Since the present model does not predict an effect of pressure on plasticity, predicted effects of pressure on swelling ratio reflect pressure effects on volatiles holdup in bubbles. At 1 atm and vacuum, the predicted swelling ratio exhibits a maximum at low peak temperatures (~600 and ~500°C, respectively), decreases as bubbles are released from the particle, and then starts to increase again at peak temperatures above 700°C, where the rate of tar cracking in bubbles becomes significant. Above 700°C, predicted swelling is reduced at vacuum than at 1 atm because faster bubble growth rates at vacuum cause more bubbles to be released from the particle, leaving less gas to expand the coal particle. At high pressures, compression reduces the total volume of gases held up in bubbles and lowers the swelling compared to the 1-atm case. The predictions in Figure 16 imply that there are optimum pressures and peak temperatures where maximum swelling is expected. Improved predictions should be attainable when more information becomes available on plasticity, vapor pressure of metaplast, initial bubble number density, and the rate of bubble generation.

At all temperatures studied, the number average molecular weight (MN) is between 0.3 and 0.35 kg/mol for 1-atm tar and is about 0.05 kg/mol higher for vacuum tar (Figures 4a and 4b). The model can predict reasonably well the MW variations of 1-atm tar with peak temperatures, but is unable to predict the decrease in molecular weight as pressure increases from 0.0001 atm to 1 atm (Oh, 1985). Evaporation of high-MW metaplast at the particle surface is enhanced at low pressures. Even though the model includes this evaporative transport at the particle surface, almost all the metaplast is vaporized into bubbles and

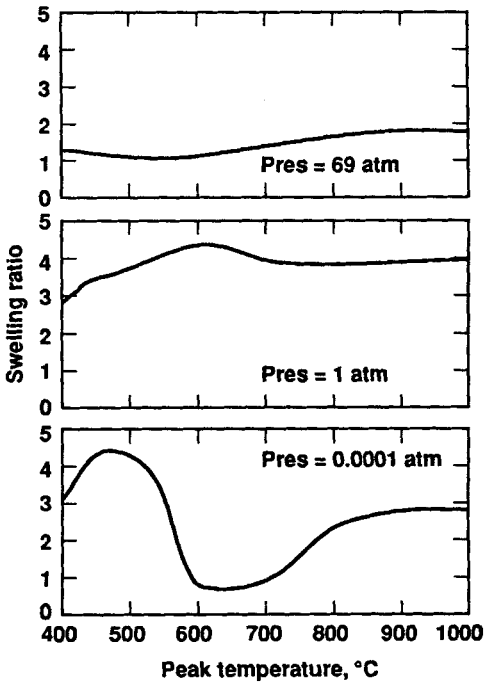

Figure 15. Model predictions of swelling ratio as a function of peak temperature at different pressures.

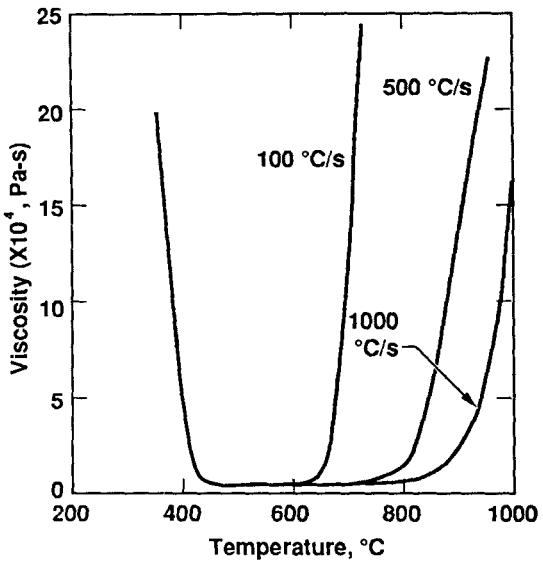

Figure 16. Heating rate effect on plastic period as coal is heated to 1,000°C at 100°C/s, 500°C/s, and 1,000°C/s at 1 atm.

leaves the particle via bubble growth, and the model does not predict the observed enhancement in high-MW metaplast yields at low pressures. The lower molecular weight of the tar from 1-atm pyrolysis may also be caused by tar cracking in bubbles and outside the particle, and by changes in the MWD of metaplast due to liquid-phase secondary reactions. Changes in the MWD of metaplast and tar are not included in the model.

The model prediction of the MW of extract was less than satisfactory. The model, however, does offer an explanation for the MW trends observed experimentally for 1-atm extract (Figure 4a). The MW of extract is the average MW of metaplast plus tar in bubbles at the time of cooling and is related to the number density of bubbles, the vapor pressure of metaplast, the rates of metaplast, and tar secondary reactions. At low temperatures, lower MW metaplast components are depleted by transport to the particle surroundings, resulting in an increase in the MW of metaplast retained in the particle. At higher temperatures, liquid-phase decomposition of metaplast is faster than decomposition of tar vapor in bubbles. During cool-down, tar vapor remaining in bubbles is condensed and extracted with the metaplast. Thus, at higher temperatures, the extractables are enriched by these lower molecular weight tars and exhibit a lower MN. Experimental data on tar and extract yields, and on MW distributions for additional pyrolysis conditions would help better understand tar and metaplast reactivity and physical properties.

Heating Rate Effects. The effects of changing heating rate from 100°C/s to 1,000°C/s on volatiles yields and on the temperature range, in which the coal is plastic, were calculated with the model. At lower heating rates more metaplast is consumed in liquid-phase secondary reactions, since coal spends more time at the relatively lower temperatures where the competing metaplast depletion process, evaporation into bubbles, is slow. At faster heating rates, coal particles are rapidly brought to temperatures where the rates of intra-particle gas and tar transport are significantly faster, causing the volatiles yields to increase. However, taking these phenomena together, the model predicted a rather small effect of heating rate on volatiles yields (Oh, 1985). For example, the predicted total volatiles yields increased by 3.4% of coal on an as-received basis, while tar increased by 2.2% (same units) at a peak temperature of 1,000°C when the heating rate was increased tenfold as noted. These predictions are not inconsistent with the experimental observations of Suuberg (1977). Suuberg observed the decrease in total weight loss of 1% when the heating rate was reduced from 1,000°C/s to a range of 350–450°C/s.

It has been experimentally observed that increasing heating rate has little effects on the coal softening point, but does shift the resolidification point to a higher temperature (Fong et al., 1986, a, b, c). The model predictions of change in plasticity under different heating rates as a function of temperature (Figure 16) are in accord with these observations.

Particle Size Effects. Figure 17 shows the model predictions of the effects of changing particle diameter on total volatiles and tar yields for pyrolysis at 1 atm at different peak temperatures. Since smaller particles have larger external surface area per unit mass available for the growing bubbles to release their volatiles from the particle, the model predicts an increase in volatiles yields as the particle size decreases. Again the model predicts the correct trend, but exaggerates the decrease in tar yield with increasing particle size as compared to the data by Suuberg et al. (1978). The spherical geometry of the model may be one of reasons for the overprediction. These calculations assumed that there were no spatial temperature gradients within the particle throughout pyrolysis. However, extension of the model to treat nonisothermal systems should present no fundamental problems, although applications to engineering calculations would involve significantly more computational complexity.

Conclusions and Significance

A new approach to quantitative modeling of volatiles mass transfer within pyrolyzing particles of softened coal was devel-

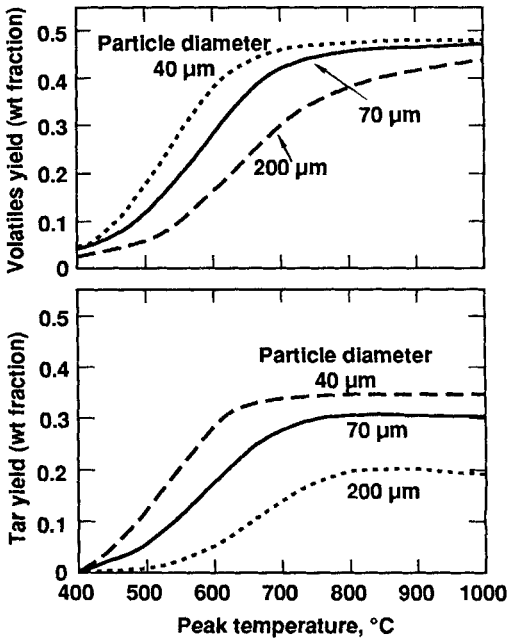

Figure 17. Model predictions of the particle size effect on total volatiles and tar yields at 1 atm.

oped and tested. The model used the following crucial concepts:

- Bubbles, uniformly distributed throughout the molten coal continuum, grow by an influx of pyrolysis volatiles.
- This bubble growth plays a major role in intraparticle transport of tar and gases.

The model predicts total weight loss and the yields of tar, gas and metaplast, and quantitatively described the physical transformations of pyrolyzing coal including swelling behavior of individual particles and the transient viscosity of the molten coal.

The model is shown to provide realistic description of important chemical and physical processes in softening coal pyrolysis. Laboratory data on yields of tars, total volatiles, and pyridine extractables of chars, as affected by temperature and time, are well correlated. Predictions of effects of pressure, particle diameter, and temperature on tar and total volatiles yields, of effects of pressure on swelling ratio, and of effects of heating rate on plastic behavior are in good qualitative accord with expectations.

Previous models have not demonstrated capability for simultaneously predicting volatiles and tar release rates, extractables yields, swelling, plasticity dynamics, and effects thereon of temperature, time, heating rate, particle size and total pressure. The last two variables are of increasing industrial importance due to expanding interest in developing and commercializing coal-fired pressurized heat engines, and pressurized equipments for electric power generation by fluidized bed combustion cycles and integrated coal gasification combined cycles.

The broad capabilities and satisfying performance of the present model arise because it accounts explicitly for:

a) Intra-particle coupling of volatiles transport and secondary reactions

b) Transient plasticity of the reacting coal

c) Intra-melt volatiles transport mechanism (namely expansion and surface escape of bubbles) that is significantly faster than liquid-phase diffusion

The encouraging agreement of the model predictions with several experimental results from this and other laboratories supports the essential validity of the modeling concepts and provides strong incentive for further research to simplify the model mathematics and obtain reliable physical and chemical property data for applications to softening coal and other thermal plastic materials.

Acknowledgment

Financial support of this work by the U.S. Department of Energy under Contract Nos. EX-76-A-01-2295 (Task Order 26), DE-AC21-82MC-19207, DE-FG22-83PC-60799, and DE-RP22-84PC-70768 is gratefully acknowledged.

Notation

a = bubble radius, m
$\dot{a} = da/dt$ = bubble growth rate, m/s
a_{pore} = pore radius, m
b_1, b_2 = constants
B_g = mass of gases in bubbles, kg/kg original coal
$B_{m,i}$ = mass of tar component i in bubbles, kg/kg original coal
C^i_{eq} = equilibrium concentration of volatile i at the interface between the molten coal and bubble phase
C_g = average concentration of gas dissolved in molten phase, kg/kg original coal
C_m = average concentration of metaplast in molten phase, kg/kg original coal
$D_{v,L}$ = diffusivity of volatiles in liquid, m^2/s
$D_{m,g}$ = diffusivity of tar in ambient gas, m^2/s
$E_{b,j}$ = escape coefficient of bubbles of size j from the particle, 1/s
E_g = escape coefficient due to gas diffusion to the particle surface, 1/s
E_m = escape coefficient due to metaplast diffusion to the particle surface, 1/s
H_r = heating rate, 1,000°C/s
k = reaction rate constant, 1/s
k_o = preexponential constants, 1/s
K_j = growth rate of bubbles of size j due to diffusion, 1/s
n_j = number of bubbles of size j per kg original coal
P = ambient pressure, atm
P_b = bubble pressure, sum of partial pressures of gases and tar, atm
P_{ij} = coagulation coefficient of between bubbles of size i and j, 1/s
P_v = vapor pressure of metaplast, atm
R_p = particle radius, m
R_{po} = particle radius at $t = 0$, m
t = time, s
T = temperature, K
v = bubble mass, kg/kg original coal
V_i^* = amount of species i formed at time $t = \infty$, kg/kg original coal
V_i = amount of species i formed at time t, kg/kg original coal
w = dimensionless bubble mass

Greek letters

ϕ = weight fraction of metaplast in coal melt
γ = dimensionless bubble radius
μ = melt viscosity, Pa · s
ρ_o = mass density of coal, kg/m^3
ρ_g = molar density of ambient gas, mol/m^3
ρ_L = molar density of coal melt, mol/m^3
σ = surface tension, N/m

Literature Cited

Anthony, D. B., "Rapid Devolatilization and Hydrogasification of Pulverized Coal," ScD Thesis, Dept. Chem. Eng., M.I.T., Cambridge, MA (1974).

Anthony, D. B., and J. B. Howard, "Coal Devolatilization and Hydrogasification," *AIChE J.*, **22,** 675 (1976).

Attar, A., "Bubble Nucleation in Viscous Material Due to Gas Formation by a Chemical Reaction, Application to Coal Pyrolysis," *AIChE J.*, **24,** 106 (1978).

Barlow, E. J., and W. E. Langlois, "Diffusion of Gas from a Liquid into an Expanding Bubble," *IBM J., Res. Dev.*, **6,** 329 (1962).

Bautistu, J. R., W. B. Russell, and D. A. Saville, "Time Resolved Pyrolysis Product Distributions of Softening Coals," *Ind. Eng. Chem. Fund.*, **25,** 536 (1986).

Bleik, A., W. M. van Poelje, W. P. M. van Swaaij, and F. P. H. van Beckum, "Effects of Intraparticle Heat and Mass Transfer During Devolatilization of a Single Coal Particle," *AIChE J.*, **31,** 1666 (1985).

Bockrath, B. C., R. B. Lacount, and R. P. Noceti, "Viscosity of Coal-derived Liquid," *Fuel Process. Technol.*, **1,** 217 (1977).

Caron, R., "Batch Reactor Manual," Internal Report, Dept. Chem. Eng. M.I.T., Cambridge, MA (1979).

Chen, L. H., and C. Y. Wen, "A Model for Coal Pyrolysis," *ACS Div. Fuel Chem. Prepr.*, **23,** 141 (1979).

Dolan, J., "Swelling and Agglomeration Effects for Bituminous Coal in a Laminar Flow Reactor," B.S. Thesis, M.I.T., Cambridge (1980).

Edwards, D., C. G. Van de Rostyne, J. Winnick, and J. M. Prausnitz, "Estimation of Vapor Pressures of High-Boiling Fractions in Liquefied Fossil Fuels Containing Heteroatoms Nitrogen and Sulfur." *Ind Eng. Chem. Proc. Des. Dev.*, **20,** 138 (1981).

Essenhigh, R. H., and G. C. York, "Reaction Rates of Single Coal Particles: Influence of Swelling, Shape, and Other Factors, *Fuel*, **44,** 177 (1965).

Fong, W. S., Y. F. Khalil, W. A. Peters, and J. B. Howard, "Plastic Behavior of Coal under Rapid-Heating High-Temperature Conditions," *ACS Div. Fuel Chem. Prepr.*, **29** (1985).
Fong, W. S., "Plasticity and Agglomeration in Coal Pyrolysis," ScD Thesis, Dept. Chem. Eng., M.I.T., Cambridge, MA (1986a).
Fong, W. S., Y. F. Khalil, W. A. Peters, and J. B. Howard, "Plastic Behavior of Coal under Rapid-Heating High-Temperature Conditions," *Fuel*, **65**, 195 (1986b).
Fong, W. S., W. A. Peters, and J. B. Howard, "Kinetics of Generation and Destruction of Pyridine Extractables in Rapidly Pyrolyzing Bituminous Coal," *Fuel*, **65**, 251 (1986c).
Frankel, N. A., and A. Acrivos, "On the Viscosity of a Concentrated Suspension of Solid Spheres," *Chem. Eng. Sci.*, **22**, 847 (1967).
Franklin, H. D., "Mineral Matter Effects in Coal Pyrolysis and Hydropyrolysis," PhD Thesis, Dept. Chem. Eng., M.I.T., Cambridge, MA (1980).
Franklin, R. E., "A study of the Fine Structure of Carbonaceous Solids by Measurements of True and Apparent Densities: Part I. Coals; Part II. Carbonized Coals," *Trans Farad. Soc.*, **45**, 274, 668 (1949).
Gan, H., S. P. Nandi, and P. L. Walker, Jr., "Nature of the Porosity in American Coals," *Fuel*, **51**, 272 (1972).
Gavalas, B. R., and K. Wilks, "Intraparticle Mass Transfer in Coal Pyrolysis," *AIChE J.*, **26**, 201 (1980).
Gelbard, F., Y. Tambour, and J. H. Seinfeld, "Sectional Representations for Simulating Aerosol Dynamics," *J. Colloid Interf. Sci.*, **76**, 541 (1980).
Grey, J. A., A. J. Brady, J. R. Cunningham, J. R. Freeman, G. M. Wilson, "Thermophysical Properties of Coal Liquids: Selected Physical, Chemical, and Thermodynamic Properties of Narrow Boiling Range Coal Liquids," *Ind. Eng. Chem. Proc. Des. Dev.*, **22**, 410
Hirsh, R. B., "X-Ray Scattering from Coals," *Proc. Roy. Soc. of Londong*, **A226**, 143 (1954).
Homann, K. H., Comment on an article by Jinno et al., *Int. Symp. on Combus.*, Cambridge (1977).
Howard, J. B., "Fundamentals of Coal Pyrolysis and Hydropyrolysis," *The Chemistry of Coal Utilization*, Ch. 12, 2nd Supple. Vol., M. A. Elliot, ed., Wiley (1981).
Hwang, S-C, L. Tsonopoulos, J. R. Cunningham, and G. W. Wilson, "Density, Viscosity, and Surface Tension of Coal Liquids at High Temperatures and Pressures," *Ind. Eng. Chem. Proc. Des. Dev.*, **21**, 217 (1982).
James, R. K., and A. F. Mills, "Analysis of Coal Particle Pyrolysis," *Lett. in Heat and Mass Transfer*, **3**, 1 (1976).
Lewellen, P. C., "Product Decomposition Effects in Coal Pyrolysis," MS Thesis, Dept. of Chem. Eng., M.I.T., Cambridge (1975).
Lowenthal, G., W. Wanzl, and K. H. Van Heek, "Kinetics of Swelling and Plasticity of Coal During Rapid Pyrolysis and Hydropyrolysis," *Fuel*, **65**, 356 (1986).
Maiorella, B. L., "Behavior of Liquid Subbituminous Coal Tars Upon Heating, as it Relates to In-Situ Gasification," BS Thesis, Dept. Chem. Eng., M.I.T., Cambridge, MA (1978).
Matsunaga, T., "Gasification of Coals Treated with Non-aqueous Solvent and Swelling Behavior of a Single Coal Particle," *Fuel*, **57**, 562 (1978).
Mills, A. F., R. K. James, and D. Antonink, *Future Energy Production Ser.* J. C. Denton and N. Afgan, eds., Hemisphere, Washington, DC (1976).
Miura, S., and P. L. Silveston, "Changes of Pore Properties during Carbonization of Coking Coal," *Carbon*, **18**, 93 (1980).
Nazem, F. F., "Rheology of Carbonaceous Mesophase Pitch," *Fuel*, **54**, 851 (1980).
Neavel, R. C., "Coal Plasticity Mechanism: Inferences from Liquefaction Studies," *Coal Sc.*, **1**, 1, M. L. Gorbaty, J. W. Larsen, and I. Wender, eds., Academic Press, New York (1982).
Oh, M. S., W. A. Peters, and J. B. Howard, "Modeling Mass Transport and Plasticity in Bituminous Coal Pyrolysis," *Int. Conf. Coal. Sci. Proc.*, Pittsburgh, PA, 483 (Aug. 15–19, 1983).
———, "Modeling Volatiles Transport in Softening Coal Pyrolysis," AIChE mtg., San Francisco (Nov. 25–30, 1984).
Oh, M. S., "Softening Coal Pyrolysis," ScD Thesis, Dept. Chem. Eng., M.I.T., Cambridge, MA (1985).
Pelofsky, A. H., "Surface Tension-Viscosity Relations for Liquids," *J. Chem. Eng. Data*, **11**(3), 394 (1966).
Reid, R., J. M. Prausnitz, and T. K. Sherwood, *Properties of Gases and Liquids*, 3rd ed., McGraw-Hill, New York (1979).
Russel, W. B., D. A. Saville, and M. I. Greene, "A Model for Short Residence Time Hydropyrolysis of Single Coal Particles," *AIChE J.*, **25**, 65 (1979).
Schaub, G., W. A. Peters, and J. B. Howard, "Rapid Hydropyrolysis of Softening Coal Particles—A Modeling Study: I. Model formulation and Parameter Values," *AIChE J.*, **31**(6), 903 (1985a); II. Model Predictions and Comparison with Experimental Results," *AIChE J.*, **31**(6), 912 (1985b).
Schiller, J. E., B. W. Farnum, and A. C. Smith, Jr., Viscosity of Coal Liquids—The Effect of Character and Content of the Non-Distillable Portion," *ACS Div. Fuel Chem., Prepr.*, **22**, 33 (1977).
Scriven, L., "On the Dynamics of Phase Growth," *Chem. Eng. Sci.*, **10**, 1 (1959).
Serio, M. A., "Secondary Reactions of Tar in Coal Pyrolysis," PhD Thesis, Dept. Chem. Eng., M.I.T., Cambridge, MA (1984).
Serio, M. A., W. A. Peters, K. Sawada, and J. B. Howard, "Secondary Reactions of Nascent Coal Pyrolysis Tars," *Int. Conf. Coal. Sci., Proc.*, Pittsburgh, PA 553 (Aug. 15–19, 1983).
Serio, M. A., W. A. Peters, and J. B. Howard, "Kinetics of Vapor Phase Secondary Reactions of Prompt Coal Pyrolysis Tar," *Ind. and Eng. Chem. Res.* **26**, 1831 (1987)
Singla, P. K., S. Muira, R. R. Hudgins, and P. L. Silveston, "Pore Development during Carbonization of Coals," *Fuel*, **62**, 645 (1983)
Sung, W. F., "The Study of the Swelling Property of Bituminous Coal," MS Thesis, Dept. Chem. Eng., M.I.T., Cambridge (1977).
Suuberg, E. M., "Rapid Pyrolysis and Hydropyrolysis of Coal," ScD Thesis, Dept. Chem. Eng., M.I.T., Cambridge (1977).
Suuberg, E. M., W.A. Peters, and J. B. Howard, "Product Compositions and Formation Kinetics in Rapid Pyrolysis of Pulverized Coal—Implications for Combustion," *Int. Symp. on Combust.* Combustion Institute, Pittsburgh, 117 (1978).
———, "Comparison of the Rapid Pyrolysis of a Lignite and a Bituminous Coal," *Thermal Hydrocarbon Chemistry*, A. G. Oblad, H. G. Davis, and R. T. Eddlinger, eds., Adv. in Chem. Ser., No. 183, ACS, Washington DC, 239 (1979).
Toda, Y., M. Hatami, S. Toyoda, Y. Yoshida, and H. Honda, "Fine Pore Structure of Carbonized Coals," *Carbon*, **8**, 565 (1970).
Tsai, C. Y., and A. W. Scaroni, "The Structural Changes of Bituminous Coal Particles during the Initial Stage of Pulverized Coal Combustion," *Fuel*, **66**, 200 (1987)
Unger, P. E., and E. M. Suuberg, "Modeling the Devolatilization Behavior of a softening Bituminous Coal," Int. Symp. on Combust., Combust. Inst., 1203 (1981).
———, "Internal and External Mass Transfer Limitations in Coal Pyrolysis," *ACS Div. Fuel Chem. Prepr.*, **28**(4), 278 (1983).
Van Krevelen, D. W., *Coal*, Elsevier, Amsterdam (1961).
Wagner, R., W. Wanzl, and K. H. van Heek, "Influence of Transport effects on Pyrolysis Reaction of Coal at High Heating Rates," *Fuel*, **64**, 571 (1985).
Wilson, G. M., J. R. H. Johnson, S-C Hwang, and C. Tsonopoulos, "Volatility of Coal Liquids at High Temperatures and Pressures," *Ind. Eng. Chem. Proc. Des. Dev.*, **20**, 94 (1981).
Yau, Y. D., J. J. Kirkland, and D. P. Bly, *Modern Size-Exclusion Liquid Chromatography*, Wiley, New York (1979).
Zacharias, M. W., "Analysis of Product Yields from Rapid Pyrolysis of Bituminous Coal," MS Thesis, Dept. Chem. Eng., M.I.T., Cambridge (1979).

Manuscript received Jan. 19 and Apr. 29, 1988, in two parts, and revision received Dec. 14, 1988.